

Effects of a Calcium-Channel Blocker (CV159) on Hepatic Ischemia/Reperfusion Injury in Rats: Evaluation with Selective NO/pO₂ Electrodes and an Electron Paramagnetic Resonance Spin-Trapping Method

Keizo HATAJI,^a Taiji WATANABE,^{*,b} Shigeru OOWADA,^a Masaki NAGAYA,^c Masato KAMIBAYASHI,^d Eiichi MURAKAMI,^e Hiroyoshi KAWAKAMI,^f Atsuko ISHIUCHI,^a Toshio KUMAI,^g Hiroshi NAKANO,^a Shinichi KOBAYASHI,^g and Takehito OTSUBO^a

^aDepartment of Gastroenterological and General Surgery, St. Marianna University Hospital; ^gDepartment of Pharmacology, St. Marianna University Hospital; 2-16-1 Sugao, Miyamae-ku, Kawasaki 216-8511, Japan:

^bHamamatsucho 1st Clinic Yokohama; Kamiya building 4F, 2-19-4 Tsuruya-cho, Kanagawa-ku, Yokohama; 221-0835,

Japan: ^cDepartment of Surgery, Pittsburgh, University of Pittsburgh; PA 15201, U.S.A.: ^dKyoto Pharmaceutical University; Yamashina, Kyoto 607-8412, Japan: ^eEikokagaku; Tokyo 156-0041, Japan: and ^fDepartment of Applied Chemistry, Tokyo Metropolitan University; 1-1 Minami-Osawa, Hachioji, Tokyo 192-0397, Japan.

Received July 13, 2009; accepted October 10, 2009; published online October 16, 2009

Nitric oxide (NO) and the partial pressure of oxygen (pO₂) in the liver were simultaneously quantified in rats with partial hepatic ischemia/reperfusion injury (PHIRI). Real-time NO/pO₂ monitoring and immunohistochemical analysis for superoxide dismutase and inducible nitric oxide synthase (iNOS) and endothelial NOS (eNOS) were performed to evaluate the protective effects of a dihydropyridine-type calcium-channel blocker—CV159—on PHIRI. Serum high-mobility-group box-1 (HMGB-1) was measured to assess cellular necrosis. Moreover, we used *in vitro/ex vivo* electron paramagnetic resonance spin trapping to assess the hydroxyl radical ($\cdot\text{OH}$)-scavenging activity (OHSA) of CV159 and the liver tissue. The NO levels were significantly higher in CV159-treated rats than in control rats throughout the ischemic phase. Immediately after reperfusion, the levels temporarily increased in waves and then gradually decreased in the treated rats but remained constant in the control rats. pO₂ was continually higher in the treated rats. In these rats, hepatic eNOS expression increased, whereas iNOS expression decreased. The treated rats exhibited significantly higher cytosolic and mitochondrial concentrations NO_x (NO₂+NO₃). The serum HMGB-1 levels significantly decreased in the treated rats. Moreover, CV159 directly scavenged $\cdot\text{OH}$ and both mitochondrial and cytosolic OHSA were preserved in the treated rats. Thus, CV159-mediated inhibition of intracellular Ca²⁺ overloading may effectively minimize organ damage and also have $\cdot\text{OH}$ -scavenging activity and the cytoprotective effects of eNOS-derived NO.

Key words hepatic ischemia/reperfusion injury; nitric oxide; endothelial nitric oxide; high-mobility-group box-1; hydroxyl radical-scavenging activity

Nitric oxide (NO) is an important bioregulatory molecule that was originally known as the endothelium-derived relaxing factor. Its effects in modulating vascular tone have been well documented.^{1–3} NO is generally known to inhibit reactive oxygen species (ROS)-mediated reactions, and its protective effects under various conditions are presumably attributable to its ability to detoxify ROS such as superoxide (O₂^{•-}) and hydroxyl radicals ($\cdot\text{OH}$) in hepatic ischemia/reperfusion (I/R) injury.^{2–4} Immediately after the initiation of reperfusion, endothelial nitric oxide synthase (eNOS) becomes dysfunctional and stops generating NO, this increases ROS production by Kupffer cells and induces neutrophil recruitment.^{4–7} However, the endogenous levels of eNOS during hepatic I/R injury have not been examined under conditions of ROS inhibition. In order to better understand the biological roles of NO, its levels should be measured under conditions of hepatic I/R injury with significant ROS suppression.⁸

We previously reported that NO and partial pressure of oxygen (pO₂) levels can feasibly be monitored under ischemic conditions in rats with I/R injury of the small bowels by using electrodes selective for NO and O₂ molecules.⁹ We have been studying the advanced treatment of hepatic I/R injury. 1,4-Dihydro-2,6-dimethyl-4-(3-nitrophenyl)-3,5-

pyridinedicarboxylic acid methyl 6-(5-phenyl-3-pyrazolyl-oxy) hexyl ester (designated as CV159), which is a 1,4-dihydropyridine derivative, represents a new class of calcium antagonists that function *via* the selective blockade of Ca²⁺/Calmodulin (Ca²⁺/CaM).^{10,11} By performing *in vivo* and *ex vivo* electron paramagnetic resonance (EPR) measurements, we found that CV159 retained its organ-reducing activity against radicals in hepatic I/R injury. In ischemic liver injury, CV159 prevents intracellular Ca²⁺ overloading and may thus effectively minimize organ damage by inhibiting ROSs.^{12,13} On the other hands, our previous study revealed that activation of high-mobility-group box-1 (HMGB-1) is involved in the immediate proinflammatory stress response to hepatic I/R injury and that treatment with an anti-HMGB-1 antibody significantly improves survival. We proposed that serum HMGB-1 levels can be clinically used as a marker of liver injury, especially in hepatocellular necrosis.¹⁴

The present study was designed to investigate the kinetics of HMGB-1 and the effects of CV159 treatment in hepatic I/R injury. We examined the organ-reducing ability of CV159 in rats by using a real-time system for simultaneously monitoring the NO concentrations, the dynamics of the pO₂, and the concentration of NO_x—the final metabolite of NO—under conditions of ROS suppression. Further, we performed

* To whom correspondence should be addressed. e-mail: twhama-1@honey.ocn.ne.jp

immunohistochemical analysis to identify the mechanisms by which CV159 maintains eNOS expression and inhibits inducible NOS (iNOS) expression in hepatic cells under conditions of I/R injury. In addition, because the $\cdot\text{OH}$ is very harmful and impairs cellular functions, we assessed the $\cdot\text{OH}$ -scavenging activity of CV159 and the live tissue by using an *in vitro* EPR spin-trapping method.

MATERIALS AND METHODS

Animals Male Sprague-Dawley rats (8–10 weeks old) were used for this study. All procedures were carried out in accordance with the guidelines of the St. Marianna University Institution Animal Care and Use Committee.

Synthesis of CV159 CV159 was synthesized according to a previously described method.¹¹ In brief, the reaction of 6-chlorohexanol with 3-phenyl-5-pyrazolone in the presence of K_2CO_3 in dimethylformamide (DMF) produces 6-(5-phenyl-3-pyrazolyloxy) hexyl alcohol. This compound in turn reacts with ammonium carbonate in refluxing methanol to produce 3-amino-crotonic acid 6-(5-phenyl-3-pyrazolyloxy) hexyl ester, which is finally cyclized with methyl 3-nitrobenzylidene acetoacetate in ethanol.

Surgical Preparation General anesthesia was induced in the rats by administering an intraperitoneal (i.p.) injection of 40 mg/kg sodium pentobarbiturate (Dainippon Pharmaceutical Co., Ltd., Osaka, Japan). The abdomen was shaved, and a midline incision extending from the xiphoid process to the pubis was made. The xiphoid process was clamped, and the thoracic and abdominal cavities were further exposed by using retractors along the sides. The bowel loops were exteriorized and placed on saline-soaked gauze to gain access to the liver and accessory structures.

Partial Hepatic I/R Injury We induced partial hepatic ischemia in the rats by maintaining ischemia for 60 min, followed by reperfusion, as described previously.¹⁵ In brief, the rats were prepared for surgery, and the portal triad (the portal vein, hepatic artery, and bile duct) was subsequently identified. We then occluded the blood flow to the median and left hepatic lobes while preserving adequate blood flow to the right and caudate lobes by placing a microvascular clamp on the respective vascular branches.

Experimental Protocol The rats were divided into a CV159-treated group and a control group. During the induction of partial hepatic I/R injury (PHIRI), the rats in the CV159-treated group were intraperitoneally administered CV159 (60 $\mu\text{g}/\text{kg}$) 1 h before clamping. The control rats were treated with an equal volume of the vehicle [phosphate-buffered saline (PBS)].

Blood Sampling Blood samples were collected in sterile heparinized tubes. The serum was separated by centrifugation at $10000\times g$ for 10 min and stored at -80°C until the assay was performed. The HMGB-1 levels were determined in blood samples collected before and 24 h after reperfusion.

In Vitro EPR Spin Trapping To measure the direct $\cdot\text{OH}$ -scavenging activity of CV159 and the liver tissue, we employed an EPR spin-trapping method. The $\cdot\text{OH}$ radical was produced by photolysis of hydrogen peroxide (H_2O_2), and the activity of CV159 in scavenging this radical was then measured by setting up a competitive reaction with the spin-trapping agent 5-(2,2-dimethyl-1,3-propoxy cyclophospho-

ryl)-5-methyl-1-pyrroline *N*-oxide (CYPMPO).¹⁶ When phosphate buffer (100 mM) solution containing 10 mM H_2O_2 and 10 mM CYPMPO (spin trap) was subjected to ultraviolet illumination for 5 s, the EPR spectrum shown in Fig. 1 was obtained. The spectrum was reproduced with the computer spectrum simulation and hyperfine splitting constants were listed in previous article.¹⁶ When CV159 was introduced into this system, the signal intensity of the CYPMPO-OH adduct decreased. For comparison, we also examined the $\cdot\text{OH}$ -scavenging activity (OHSA) of nicardipine—a known calcium antagonist. For measurement of OHSA in mitochondrial and cytosolic fractions of the liver, tissue samples were treated by the method described following part. The measurement of the hydroxyl radical scavenging activity was based on the competitive reaction between CPMPO and the sample for scavenging $\cdot\text{OH}$. The hydroxyl radical scavenging activity was expressed as reduced glutathione (GSH; Sigma Chemical, St. Louis, MO, U.S.A.) concentration equivalent (mM/mg proteins) using the standard curve of GSH. Linear correlation between OH radical peak height (4th or 5th signal peak height used) and GSH concentration was obtained (data not shown). EPR conditions were as follows; magnetic fields 336.2 ± 7.5 mT, modulation width 1.0×0.1 mT, microwave power 6 mW, time constant 0.1 s, and scanning time 2 min.

Electrodes and Measurement Instruments The NO levels and pO_2 were measured using novel NO- and pO_2 -selective microelectrodes that were developed in our laboratory for the real-time monitoring of NO levels and pO_2 . In designing a working microelectrode, we combined a commercially available NO-selective microelectrode (NOE-47; Eikoukagaku, Tokyo, Japan) and an amperometric oxygen microelectrode (POE-20W, Eikoukagaku). The respective counter electrodes employed are commercially available (NOR-20 and POR-10DEK, Eikoukagaku). The principle of the method used is as described previously.^{9,17} NO and oxygen diffuse through the gas-permeable membranes of the working electrodes and are oxidized at the electrodes, thus generating electrical current. The redox currents between the working and counter electrodes were detected using a current–voltage converter circuit, an NO meter (NO-502, Eikoukagaku), and a pO_2 meter (PO₂-150S, Eikoukagaku). The currents were recorded on a data acquisition system (PowerLab/8sp; ADInstruments Pty, Castle Hill, NSW, Australia) connected to a computer (Chart software program, ver. 5.4.1; ADInstruments Pty). The electrodes were calibrated daily before each experiment. 1-Hydroxy-2-oxo-3-(*N*-methyl-3-aminopropyl)-3-methyl-1-triazene (NOC-7) was diluted to 50, 100, and 200 μM in an aqueous solution of 0.1 N NaOH and immediately used as an NO donor. A calibration curve was plotted by measuring the current generated when NOC-7 was added to Krebs-4-(2-hydroxyethyl)-1-piperazineethanesulfonic acid (HEPES) solution. The electrode currents generated with various concentrations of NO and NOC-7 were plotted on the X and Y axes, respectively. The final standard curve for NOC-7 was expressed in terms of pA and μM . The NO- pO_2 microelectrode was calibrated to a pO_2 value of 150 mmHg in Krebs-HEPES solution under atmospheric pressure.

NOx Measurement Cytosolic and mitochondrial fractions of rat liver were prepared according to previously described methods.^{12,13} In brief, 10 volumes of homogenization buffer A (0.25 M sucrose, 100 (50) mM Tris-HCl (pH 7.4),

0.1 mM EDTA-2Na, and a protease inhibitor) were added to frozen rat liver samples, and the tissue was homogenized for 30 s in an ultrasonic homogenizer. The homogenate was filtered through a nylon mesh and centrifuged at $50\times g$ for 10 min at 4 °C. The supernatant was collected, an equal volume of homogenization buffer B (0.34 M sucrose, 100 (50) mM Tris-HCl (pH 7.4), 0.1 mM EDTA-2Na, and a protease inhibitor) was gently added to it, and the solution was centrifuged at $700\times g$ for 10 min to remove the nuclear components.¹⁸⁾ The supernatant was further centrifuged at $8000\times g$ for 10 min to separate the mitochondrial fraction, and the supernatant thus obtained was centrifuged at $100000\times g$ for 60 min to obtain the cytosolic fraction. The NO_x concentrations in both the mitochondrial and cytosolic fractions were determined using a NO_x Visible Detector/S-3210 system (Tokyo Kasei Kogyo, Tokyo, Japan).

Immunohistochemical Analysis The liver tissue specimens were fixed in 10% phosphate-buffered formalin, dehydrated, and embedded in paraffin. Further 5- μ m sections were cut and stained with hematoxylin and eosin. For immunohistochemical analysis of iNOS and eNOS, the sections were treated with anti-iNOS and anti-eNOS polyclonal antibodies (1 : 100; Santa Cruz Biotechnology, Santa Cruz, CA, U.S.A.) and stained using an En Vision kit (Dako, Tokyo, Japan). The iNOS-positive regions were observed under a Leica DM3000 optical microscope. For each rat, 20–30 sections were randomly selected, and iNOS expression was quantified using a digital image analysis software program (Leica QWin V3). iNOS expression was calculated as a percentage of the area with positive iNOS staining to the area of the whole section. Further, eNOS expression was quantified in a similar manner.

HMGB-1 Measurement For measuring HMGB-1 expression, rat serum was diluted 5-fold with PBS containing 1% casein-Na (pH 7.4). A complex of bovine HMGB-1 and HMGB-2 (hereafter referred to as HMGB-1/2) was used as a standard and was serially diluted from 200 to 0 ng/ml (specific dilutions: 200, 100, 50, 25, 12.5, 6.3, 3.1, and 0 ng/ml).

The standard dilutions and samples were introduced into solid-phase microtiter plates (100 μ l/well) coated with an anti-HMGB-1 monoclonal antibody (clone FBH7). The reaction was allowed to proceed for 1 h at room temperature. The plates were then washed 4 times with PBS, and rabbit anti-HMGB-1/2 antibodies adjusted with PBS containing 1% γ -globulin (pH 7.4) were added to the plates (100 μ l/well); this reaction was allowed to proceed for 1 h at room temperature. The plates were then washed 4 times with PBS, and peroxidase-labeled anti-rabbit IgG (H+L) was added to the plates (100 μ l/well). The plates were incubated for 1 h at room temperature and then washed 4 times with PBS. Next, tetramethylbenzidine (TMB) was added to the plates (100 μ l/well) and allowed to react for 30 min at room temperature; the reaction was arrested by adding 2 N sulfuric acid (100 μ l/well). The HMGB-1 concentrations in the samples were then determined by comparison with the standard curve.¹⁴⁾

Statistical Analysis All data were stored and statistically analyzed using the Statistical Analysis System. The results are expressed as the means \pm standard deviation (S.D.). Groups were compared by performing nonparametric ANOVA, depending on the type of variable. Significance was assumed at $p < 0.05$.

RESULTS

Survival Rate after PHIRI The postoperative survival rate was 100% in both the control and CV159-treated groups.

\cdot OH Radical-Scavenging Activity A typical \cdot OH radical adduct was obtained by photolysis of H₂O₂ solution (Fig. 1; blank). This spectrum consists of two identical groups of lines which are split by a large hyperfine coupling with phosphorus 31. The spectrum was reproduced with the computer spectrum simulation using following hyperfine splitting constants (A_N ; 1.37/1.35, A_H ; 1.37/1.23, A_P ; 4.88/4.70, respectively). CV159 could scavenge the \cdot OH radical when used at a concentration of 15 mmol/mg protein. In contrast, nicardipine did not exhibit \cdot OH-scavenging activity even at a con-

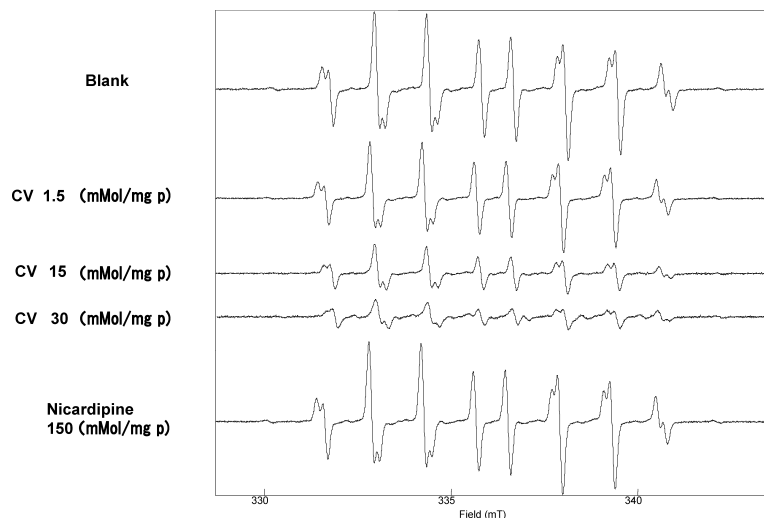


Fig. 1. \cdot OH-Scavenging Activity

A typical \cdot OH radical adduct was obtained by photolysis of H₂O₂ solution (blank). This spectrum consists of two identical groups of lines which are split by a large hyperfine coupling with phosphorus 31. The spectrum was reproduced with the computer spectrum simulation using following hyperfine splitting constants (A_N ; 1.37/1.35, A_H ; 1.37/1.23, A_P ; 4.88/4.70, respectively). CV159 exhibited \cdot OH-scavenging activity when used at a concentration of 15 mmol/mg protein, while nicardipine did not exhibit such activity even when used at a concentration of 150 mmol/mg protein. The \cdot OH-scavenging activity of CV159 was dose dependent.

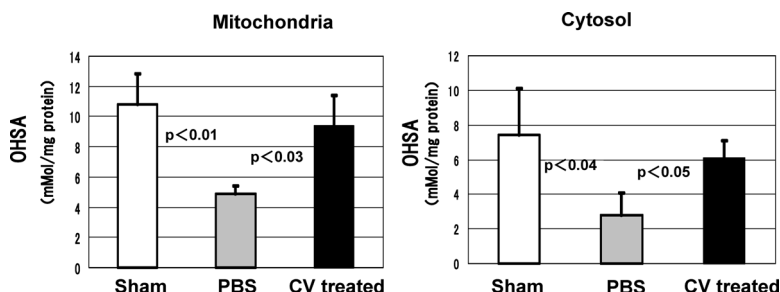


Fig. 2. Mitochondrial and Cytosolic OHSA in the 24 h after Reperfusion

OH radical scavenging activity in the liver mitochondrial and cytosolic fractions after 24 h experiment. OHSA were expressed as GSH concentration equivalent (nmol/mg proteins).

centration of 150 mmol/mg protein. Mitochondrial and cytosolic OHSA were decreased in control rats while they were preserved in CV159-treated rats (Fig. 2).

Real-Time Monitoring of NO Levels, pO_2 , and NOx Levels in the Liver The NO levels (pA) in the control group at various time points were as follows: baseline, 1863.8 ± 697.9 ; after clamping, 1696.8 ± 375.5 ; before declamping, 1127.5 ± 125.3 ; and after declamping, 1799.5 ± 486.2 . The levels in the CV159-treated group were as follows: baseline, 3437.5 ± 298.3 ; after clamping, 2064.5 ± 428.6 ; before declamping, 2908 ± 835.4 ; and after declamping, 4363.3 ± 1420.8 .

The pO_2 (mmHg) values in the control group at various time points were as follows: baseline, 8.37 ± 2.72 ; after clamping, 4.73 ± 2.26 ; before declamping, 4.63 ± 1.65 ; and after declamping, 5.30 ± 2.45 . The values in the CV159-treated group were as follows: baseline, 17.40 ± 8.96 ; after clamping, 14.88 ± 9.22 ; before declamping, 18.37 ± 12.48 ; and after declamping, 29.93 ± 8.39 .

The NO levels and pO_2 in the liver were simultaneously monitored. In the PBS-treated controls, the NO levels remained constant throughout the measurement, and the pO_2 current decreased after clamping. The NO level at baseline was significantly higher in the CV159-treated group than in the control group. In the CV159-treated group, the NO level decreased soon after clamping, remained constant under ischemic conditions, and was significantly higher than that in the control group just before unclamping. Immediately after reperfusion, the NO level in the CV159-treated group temporarily increased in a wave-like manner and then gradually decreased. After a momentary time lag, pO_2 similarly began to increase in a wave-like manner (Fig. 3).

NOx Concentrations The cytosolic NOx level in the CV159-treated group (2.33 ± 0.63 nmol/mg protein) was lower than that in the control group (3.58 ± 0.27 nmol/mg protein) and almost equal to that in the sham group (1.31 ± 0.21 nmol/mg protein; Fig. 4). The mitochondrial NOx level in the CV159-treated group (9.37 ± 0.17 nmol/mg protein) was considerably lower than that in the control group (18.69 ± 0.54 nmol/mg protein) and slightly lower than that in the sham group (6.94 ± 0.28 nmol/mg protein; Fig. 4).

Pathological and Immunohistochemical Findings In the CV159-treated group, the liver samples exhibited strong positive staining with the anti-superoxide dismutase (SOD) and anti-eNOS antibodies and weak staining with the anti-iNOS antibody. In contrast, the control group samples exhibited weak staining with the anti-eNOS antibody and strong

staining with the anti-iNOS antibody (Fig. 5).

Assessment of Hepatocellular Injury To determine whether CV159 has protective effects against hepatic I/R injury, we administered this agent to rats with induced hepatic I/R injury. In the control group, the serum HMGB-1 levels at 6 and 24 h after reperfusion were significantly higher than those at baseline. Further, the levels at 24 h after reperfusion were significantly lower in the CV159-treated group than in the control group. The serum HMGB-1 level in the sham group was 3.0 ± 1.42 μ g/ml. In the control group, the levels were 2.48 ± 1.25 and 9.86 ± 2.64 μ g/ml at 6 and 24 h after reperfusion, respectively ($p < 0.01$). In the CV159-treated group, the levels were 2.64 ± 1.93 and 2.25 ± 1.35 μ g/ml at 6 and 24 h after reperfusion, respectively (Fig. 6).

DISCUSSION

CV159 represents a new class of calcium antagonists that function by selective blockade of Ca^{2+} /CaM. Previous studies have shown that CV159 at a micromolar-order concentration inhibits the expression of Ca^{2+} /CaM-activated myosin light chain kinase (MLCK); however, it does not inhibit trypsin-treated MLCK, which is active in the absence of Ca^{2+} /CaM.^{10,11} Moreover, the precise role of CaM in intracellular signaling has gradually been elucidated. Large increases in the free Ca^{2+} concentration in the cytosol activate several kinases that are important for neural plasticity, including Ca^{2+} /CaM-dependent kinase II (CaM II), protein kinase A (PKA), and protein kinase C (PKC). Further, O_2^- is known to activate these kinases, mainly in non-neuronal systems, and O_2^- production in the mitochondria partly proceeds independent of $[Ca^{2+}]$.^{10,11} We reported that CV159 exhibits considerable organ-reducing activity in hepatic I/R injury using an *in vivo* and *ex vivo* EPR technique with a spin probe.^{12,13}

NO, especially when present in excess, is cytotoxic and causes lipid peroxidation, peroxynitrite ($ONOO^-$) formation, and the inhibition of mitochondrial respiration.^{19–22} In the late stages of reperfusion, activation of iNOS in Kupffer cells, neutrophils, and hepatocytes drastically increases the production of NO, causing injury to the surrounding cells.^{4,8} Conversely, eNOS-derived NO may exert protective effects in models of I/R injury by inducing vasodilation and enhancing perfusion in posts ischemic tissue.^{1–3} However, because NO is extremely labile and difficult to measure independently, its role and dynamics in the pathogenesis of hepatic I/R injury have not been fully elucidated.

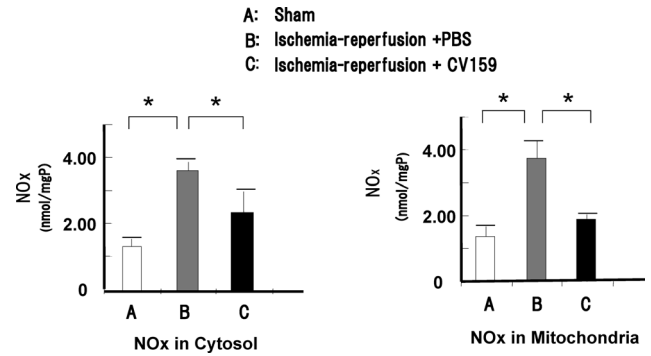
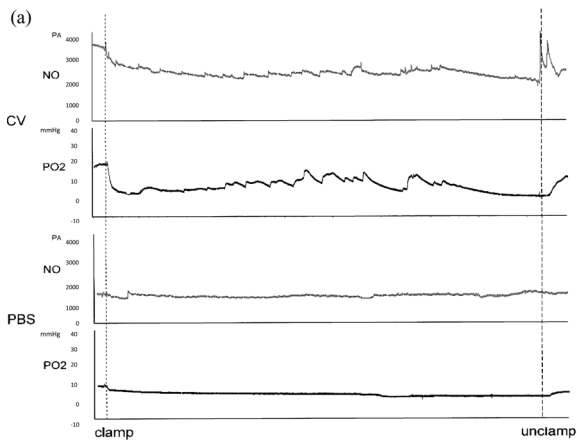


Fig. 4. Hepatic NOx Levels (nmol/mg protein) 24 h after Reperfusion

NOx levels in the sham group (open bars), the group with induced I/R (gray bar), and the group with induced I/R and CV159 treatment (filled bars). The level in the CV159-treated group was lower than that in the control group and almost equal to that in the sham group. Data are presented as the means±S.D. Each group contained 6 animals. * $p < 0.01$.

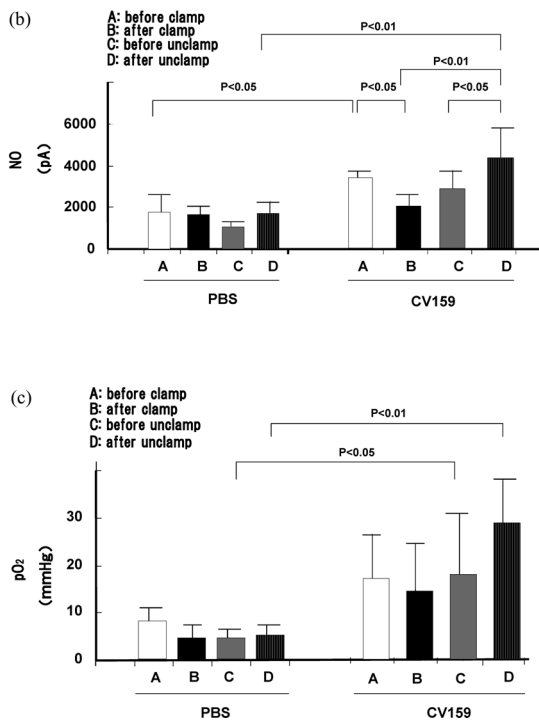


Fig. 3. (a) Representative Chart of Hepatic NO and pO_2 Levels in CV159 and PBS Treated Rat

A typical graph showing the real-time dynamics in the 2 groups. In the PBS-treated controls, the NO level remained constant. The pO_2 current decreased after clamping. The NO level at baseline was significantly higher in the CV159-treated group than in the control group. The NO level temporarily increased in a wave-like manner immediately after clamping and was then restored to the baseline level. Immediately after reperfusion, the NO level temporarily increased in a wave-like manner and then gradually decreased. After a momentary time lag, pO_2 began to increase in a wave-like manner.

(b) Hepatic NO Levels in CV159 and PBS Treated Rats

The NO levels (pA) in the control group at various time points were as follows: baseline, 1863.8 ± 697.9 ; after clamping, 1696.8 ± 375.5 ; before declamping, 1127.5 ± 125.3 ; and after declamping, 1799.5 ± 486.2 . The levels in the CV159-treated group were as follows: baseline, 3437.5 ± 298.3 ; after clamping, 2064.5 ± 428.6 ; before declamping, 2908 ± 835.4 ; and after declamping, 4363.3 ± 1420.8 . NO levels in the control and CV159-treated groups at 4 time points (before clamping, after clamping, before unclamping, and after unclamping). Data are presented as the means±S.D. Each group contained 4 animals.

(c) Hepatic pO_2 Levels in CV159 and PBS Treated Rats

The pO_2 (mmHg) values in the control group at various time points were as follows: baseline, 8.37 ± 2.72 ; after clamping, 4.73 ± 2.26 ; before declamping, 4.63 ± 1.65 ; and after declamping, 5.30 ± 2.45 . The values in the CV159-treated group were as follows: baseline, 17.40 ± 8.96 ; after clamping, 14.88 ± 9.22 ; before declamping, 18.37 ± 12.48 ; and after declamping, 29.93 ± 8.39 . pO_2 in the control and CV159-treated groups at 4 time points (before clamping, after clamping, before unclamping, and after unclamping). Data are presented as the means±S.D. Each group contained 4 animals.

In the present study, we gained some novel insights into the action mechanism of CV159 administered after hepatic I/R injury. First, we studied the real-time dynamics of NO in rats with hepatic I/R injury, under conditions of ROS suppression. During the ischemic phase of PHIRI, the NO level was significantly higher in the CV159-treated rats than in the control rats at all time points considered. Immediately after reperfusion, the NO level temporarily increased in a wave-like manner and then gradually decreased in the CV159-treated group but did not change noticeably in the control group. Moreover, immunohistochemical analysis revealed that at 24 h after reperfusion, eNOS expression in the liver samples was markedly higher, and the iNOS expression significantly lower, in the CV-treated group than in the control group. These findings suggest that CV159 can increase NO production through eNOS activation. Studies have revealed that some dihydropyridine-type calcium-channel antagonists, such as amlodipine, exert vasodilative effects by activating eNOS and inhibiting the production of the superoxide anion radical ($O_2^{\cdot-}$).^{21,23,24} Secondly, in our *in vitro* experiments, CV159 exhibited $\cdot OH$ -scavenging activity in a dose-dependent manner. In the early stage of PHIRI, both NO production and the $\cdot OH$ -scavenging activity of CV159 may have beneficial effects: The superoxide anion radical reacts with NO to produce peroxynitrite, thus yielding a highly toxic species such as the hydroxyl radical ($\cdot OH$)—the start point of lipid peroxidation and/or endothelial injury. We also found that CV159 directly scavenged the $\cdot OH$ radical *in vitro* and both mitochondria and cytosolic OHSAs in the liver were preserved in CV-159 treated rats. Thirdly, we measured the concentrations of NOx—the final metabolite of NO—in cytosolic and mitochondrial fractions of rat liver. Interestingly, we found that at 24 h after reperfusion, these concentrations in the CV159-treated group were significantly lower than those in the control group and almost equal to those in the sham group. iNOS is known to produce NO in large amounts. Our results suggest that CV159 exerts protective effects against the toxicity of iNOS-derived NO. In our previous study, we found that the superoxide-scavenging activity (SSA) in CV159-treated rats was higher than that in untreated rats and almost equal to that in a sham group of rats.^{12,13} In the present study, the observed increase in the NOx levels and SOD in the liver indicated the protective effects of CV159 on cells.

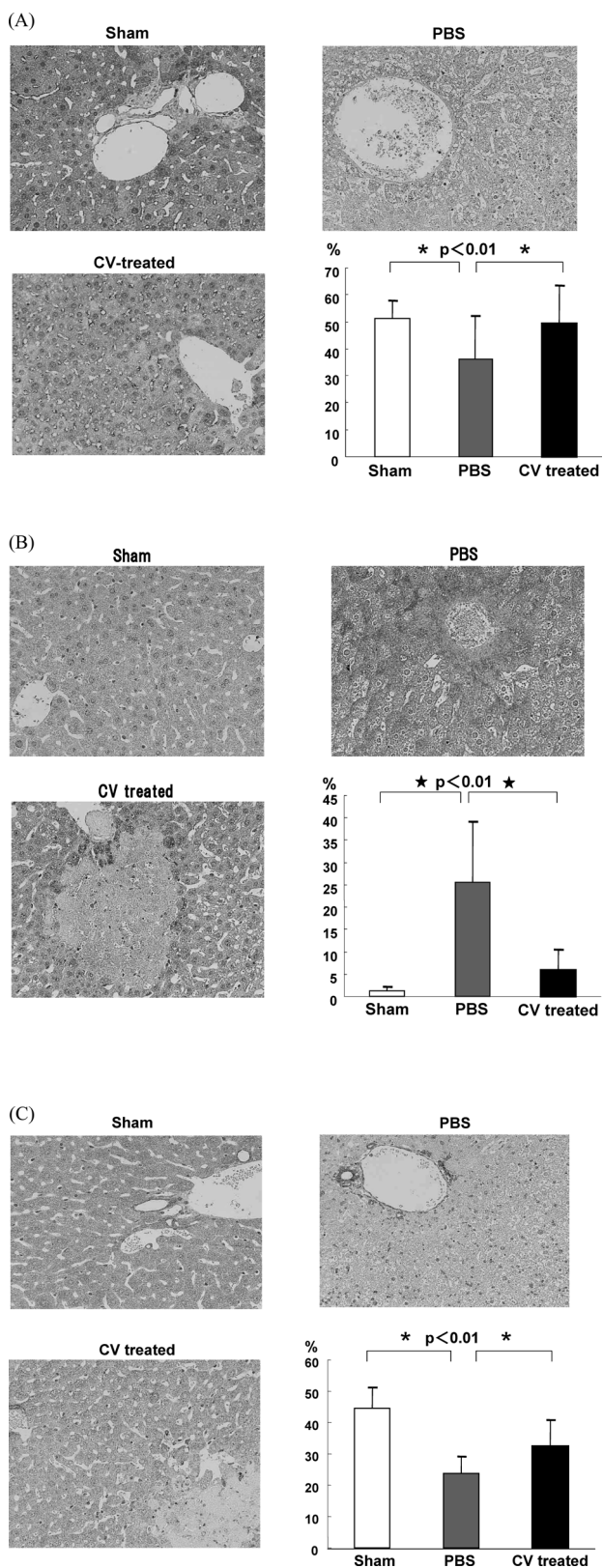


Fig. 5. (A) Immunostaining for Anti-SOD Antibody in the Liver (×200)
 SOD expression in the liver was lower in the control group than in the sham and CV-treated groups.
 (B) Immunostaining for Anti-iNOS Antibody in the Liver (×200)
 iNOS expression in the liver was lower in the sham and CV159-treated groups than in the control group.
 (C) Immunostaining for Anti-eNOS Antibody in the Liver (×200)
 eNOS expression in the liver was higher in the sham and CV159-treated groups than in the control group.

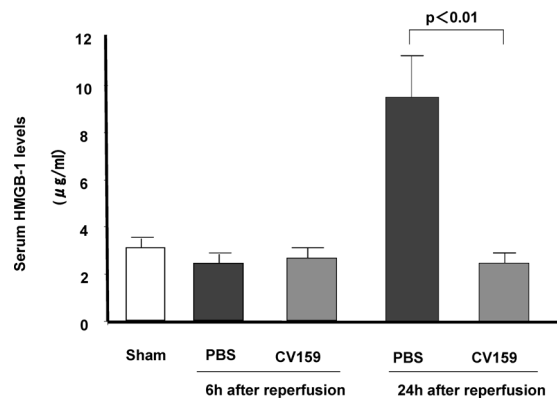


Fig. 6. Serum HMGB-1 Levels (µg/ml)
 The HMGB-1 level in the sham group was 3.0±1.42 µg/ml. At 6 and 24 h after reperfusion, the serum HMGB-1 levels were 2.48±1.25 and 9.86±2.64 µg/ml, respectively, in the control group ($p<0.01$) and 2.64±1.93 and 2.25±1.35 µg/ml, respectively, in the CV159-treated group. At 24 h after reperfusion, the serum HMGB-1 level in the control group was significantly higher than that in the CV159-treated group ($p<0.01$). Data are presented as the means±S.D. Each group contained 6 animals. * $p<0.01$.

Although the NO level was significantly high in the CV159-treated rats, NOx production was reduced. Thus, a small amount of NO appears to have reacted with O_2^- to form peroxynitrite ($ONOO^-$), because CV159-induced ROS suppression inhibited O_2^- formation. Finally, however HMGB-1 has recently received increasing attention as a late mediator of endotoxin lethality, we previously demonstrated that systemic accumulation of HMGB-1 occurs within 24 h after hepatic I/R injury.¹⁴ In the present study, we found that (1) HMGB-1 expression exhibited time-dependent kinetics in hepatic I/R injury in rats and (2) at 24 h after reperfusion, the serum HMGB-1 levels were significantly lower in the CV159-treated group than in the control group.

Ischemic postconditioning—a novel strategy involving the Pringle maneuver (clamping of the portal pedicle)—is commonly used to occlude the blood flow to the liver during surgery.²⁵ The implicated factors include ROS generation, leukocyte migration and activation, microcirculatory abnormalities, and sinusoidal endothelial cell damage.²⁵ Pharmacological postconditioning, which involves the administration of an agent that mediates the protective effects of postconditioning, is a more practical option, and CV159 might be used as an adjuvant in the Pringle maneuver.¹³ Further clinical studies would shed light on the potential clinical applications of CV159 as a pharmacological postconditioning agent in the Pringle maneuver.

In conclusion, the results of this study reveal that in hepatic I/R injury, CV159-mediated inhibition of intracellular Ca^{2+} overloading may effectively minimize organ damage and have also both (1) hydroxyl-scavenging activity and (2) the cytoprotective effects of eNOS-derived NO.

REFERENCES

- Lu P., Liu F., Wang C. Y., Chen D. D., Yao Z., Tian Y., *World J. Gastroenterol.*, **11**, 3441—3445 (2005).
- Hisamoto K., Ohmichi M., Kurachi H., Hayakawa J., Kanda Y., Nishio Y., *J. Biol. Chem.*, **276**, 3459—3467 (2001).
- Haynes M. P., Sinha D., Russell K. S., Collinge M., Fulton D., Morales-Ruiz M., *Circ. Res.*, **87**, 677—682 (2000).
- Liu P., Yn K., Nagele R., Wong P. Y., *J. Pharmacol. Exp. Ther.*, **284**,

- 1139—1146 (1998).
- 5) Jaeschke H., *Chem. Biol. Interact.*, **79**, 115—136 (1991).
 - 6) Hidemasa K., Makiya N., Fumiyoshi Y., Mitsuru H., *Transplantation*, **85**, 264—269 (2008).
 - 7) Fleming I., Busse R., *Am. J. Physiol. Regul. Integr. Comp. Physiol.*, **284**, R1—R12 (2003).
 - 8) Lee V. G., Johnson M. L., Baust J., Laubach V. E., Watkins S. C., Billiar T. R., *Shock*, **16**, 355—360 (2001).
 - 9) Watanabe T., Owada S., Kobayashi H., Ishiuchi A., Nakano H., Asakura T., *Transplant. Proc.*, **39**, 3007—3009 (2007).
 - 10) Umekawa H., Yamakawa K., Kazuo N., Norio T., Tanaka T., Hidaka H., *Biochem. Pharmacol.*, **37**, 3377—3381 (1988).
 - 11) Miyazaki H., Tanaka S., Fujii Y., Shimizu K., Nagashima K., Kamibayashi M., *Life Sci.*, **64**, 869—878 (1999).
 - 12) Watanabe T., Owada S., Kobayashi H. P., Kamibayashi M., Ishiuchi A., Jinnouchi Y., *J. Surg. Res.*, **145**, 49—56 (2008).
 - 13) Kobayashi H. P., Watanabe T., Owada S., Hirayama A., Nagase S., Kamibayashi M., *J. Surg. Res.*, **147**, 41—49 (2008).
 - 14) Watanabe T., Kubota S., Nagaya M., Ozaki S., Nagafuchi H., Akashi K., *J. Surg. Res.*, **124**, 59—66 (2005).
 - 15) Kohli V., Madden J. F., Bentley R. C., Clavien P. A., *Gastroenterology*, **116**, 168—178 (1999).
 - 16) Kamibayashi M., Owada S., Kameda H., Okada T., Inanami O., Ohta S., *Free Radic. Res.*, **40**, 1166—1172 (2006).
 - 17) Yomura Y., Shoji Y., Asai D., Murakami E., Ueno S., Nakashima H., *Life Sci.*, **80**, 1449—1457 (2007).
 - 18) Verdon C. P., Burton B. A., Prior R. L., *Anal. Biochem.*, **224**, 502—508 (1995).
 - 19) Ijaz S., Yang W., Winslet M. C., *Microvasc. Res.*, **70**, 129—136 (2005).
 - 20) Matsubara M., Yao K., Hasegawa K., *Pharmacol. Res.*, **53**, 35—43 (2006).
 - 21) Batova S., DeWever J., Godfraind T., Balligand J. L., Dessy C., Feron O., *Cardiovasc. Res.*, **71**, 411—413 (2006).
 - 22) Moncada S., Palmer R. M., Higgs E. A., *Pharmacol. Rev.*, **43**, 109—142 (1991).
 - 23) Catalioto R. M., Renzetti A. R., Criscuoli M., Morbidelli L., Subissi A., *J. Cardiovasc. Pharmacol.*, **127**, 195—200 (1996).
 - 24) Chen L., Haught W. H., Yang B., Saldeen T. G., Parathasarathy S., Mehta J. L., *J. Am. Coll. Cardiol.*, **30**, 569—575 (1997).
 - 25) Kucuk C., Akcan A., Akylyz H., Akgun H., Muhtaroglu S., Sozuer E., *J. Surg. Res.*, **15**, 74—79 (2009).